

**2019 NDIA GROUND VEHICLE SYSTEMS ENGINEERING AND TECHNOLOGY
SYMPOSIUM
MSTV TECHNICAL SESSION
AUGUST 13-15, 2019 - Novi, Michigan**

**THE EFFECTS OF OBSTACLE DIMENSIONAL UNCERTAINTY ON
PATH PLANNING IN CLUTTERED ENVIRONMENTS**

**Seth Tau^{1,2}, Sean Brennan, PhD¹, Karl Reichard, PhD², Jesse Pentzer, PhD²,
David Gorsich, PhD³**

¹Department of Mechanical Engineering, Penn State University, State College, PA

²Applied Research Laboratory, Penn State University, State College, PA

³U.S. Army CCDC Ground Vehicle Systems Center, Warren, MI

ABSTRACT

This work investigates the effects of obstacle uncertainty on the speed, distance, and feasibility of a planned traversal path. Simulation results for artificial and real-world environments are used to numerically quantify how geometric uncertainty within a map affects path traversal cost. A significant outcome of this research is the discovery of a relationship between increasing uncertainty and path cost. As obstacle uncertainty increases, previously planned routes can become infeasible as they effectively become blocked off due to uncertainty in the obstacle geometry. This paper illustrates a method that can serve to increase the speed, simplicity, and reliability of path planning, while allowing uncertainty to be included in the mobility analysis.

Citation: S. Tau, S. Brennan, K. Reichard, J. Pentzer, D. Gorsich, “The Effects of Obstacle Dimensional Uncertainty on Path Planning in Cluttered Environments”, In *Proceedings of the Ground Vehicle Systems Engineering and Technology Symposium (GVSETS)*, NDIA, Novi, MI, Aug. 13-15, 2019.

1. INTRODUCTION

The U.S. Army has been using the NATO Reference Mobility Model (NRMM) to inform path-planning decisions since the 1970s. The main use for NRMM has been to compare vehicle designs and determine the mobility of vehicles under certain terrain conditions. Although this tool has been a valuable asset over the years, it does not take into account many modern vehicle characteristics [1-3] or the uncertainty inherent with any real-world vehicle and environment [3,4].

Recently there have been efforts to modernize and update the NRMM [1-4], and one specific intent for the Next Generation NRMM (NG NRMM) is to include factors for modeling vehicle and environmental uncertainty [3,4]. Choi, et al. has focused on accounting for what they call irreducible uncertainty in the environment [4,5] while others, including Ghiocel et al. have focused on reducible uncertainty within the vehicle [6]. This paper is interested in reducible uncertainty in environmental factors. Specifically, the analysis presented here will focus on the dimensional uncertainty of obstacles.

In this paper, global knowledge of obstacle position and general geometric shape will be assumed, but the extent of the dimensions will be assumed to be uncertain. That is, the global location of each obstacle is known, but the actual size of the obstacle is not known for certain. This type of uncertainty can be represented by dilating the ground truth obstacle to reach the assumed size, as shown in figure 1 and explained in section 2.

In order to make this analysis easily extendable to environments of various sizes and differing unit systems, two unitless ratios will be defined that describe the two key factors: the dimensional uncertainty and the cost of traversal. The dimensional uncertainty ratio for this paper will be defined as the average maximum radius of all the expanded obstacles divided by the average maximum radius of all the ground truth obstacles. This provides a metric for determining a percentage of overall size increase, allowing the analysis to be valid on any scale. Although other definitions could be used, the major outcomes of this paper should be the same.

The cost used in this paper will be traversal distance. The cost ratio will be defined as the total path distance divided by the Euclidean distance from the starting point to the goal point. This provides an easy way to determine how far a vehicle will actually need to travel if the Euclidean distance and cost ratio are known ahead of time. For example, if the goal point is 5 miles away and the cost ratio to travel through this environment is 1.1, then the actual travel distance should be 5.5 miles, which could be crucial information when planning an operation.

2. SIMPLIFICATIONS

For the simulations in this paper, the analysis was made tractable by several methods. First, the area of interest is represented via a visibility graph on a two-dimensional map. The map is constrained to two dimensions to simplify the analysis, but could be extended to three dimensions if desired. The visibility graph was first formalized by

Lozano-Pérez and Wesley in 1979 [7], although they state the idea predated their work [7-9]. The method is to represent all obstacles as polytopes with a finite (and ideally small) number of vertices. A visibility graph is then composed of all the connections between vertices that can be connected without passing through the interior of any obstacle and the start and goal points, with some cost to move between each pair [7]. This type of representation is useful because the shortest path around the objects will always be the shortest path between the start and goal points through the visibility graph [7].

Second, each potential obstacle is represented as a convex polytope. This requirement ensures that the path planners do not get caught in local minima. This is especially relevant to path planners using heuristics, like A*, which speed up the path planning process by making approximations of future cost [10]. This requirement can be relaxed with certain modifications to the planning algorithm, but will be kept for now to increase simplicity.

The third simplification is to dilate obstacles to account for the vehicle size and dilate again to account for uncertainty. In order for the visibility graph to be effective, the vehicle must be approximated as a point, which requires that the obstacles be extended to account for the vehicle dimensions or clearance [7]. Since the orientation of the vehicle changes as it moves throughout the map, the simplest solution is to find the radius of a circle that encompasses the vehicle and dilate each ground truth obstacle by that distance. Then the point moving along the path will represent the centroid of the vehicle. This is shown in figure 1, and ensures that as long as the centroid of the vehicle remains outside the dilated obstacle, the vehicle will never be able to contact the ground truth obstacle. On large scales this dilation is often very minute as can be seen in figure 3. Similarly, if the exact dimensions of an obstacle are only known to $\pm 10\%$ the worst-case scenario would be to take the nominal obstacle and dilate it by 10%. For this

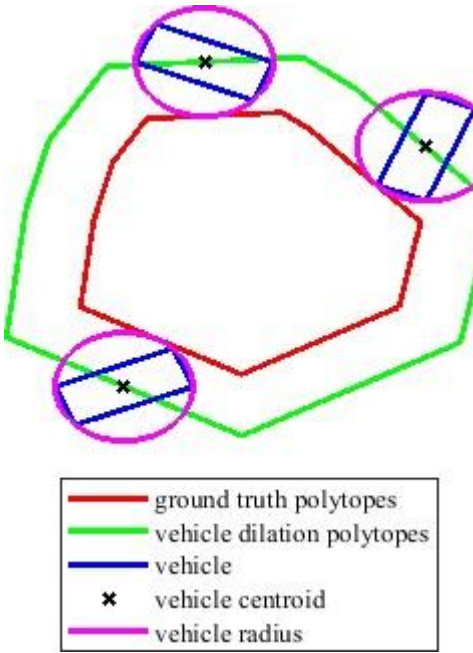


Figure 1: Example showing how polytope dilation prevents vehicles from intersecting the ground truth polytope.

analysis, this uncertainty will be implemented by doing additional dilation after the ground truth obstacle is dilated to account for vehicle size.

The final simplification is implemented to maintain convexity as more uncertainty is added to the environment. As obstacle dimensions become more uncertain, obstacles begin to overlap, which can create obstacle combinations that appear concave to path planners. In order to prevent this, whenever two or more obstacles begin to overlap, they are combined into a single convex polytope, maintaining simplification two. This can sometimes remove legitimate paths from the visibility graph and as with the second simplification, this can also be relaxed with some modification, but will be kept for simplicity.

3. SIMULATION METHOD

The analysis presented here use Dijkstra's algorithm as the path planner for determining the optimal-distance path between two points within a predefined map [11]. Dijkstra's algorithm is often slower than many heuristic algorithms. However,

since it does not consider any heuristics, it does not struggle with the local minima and, given enough time, it can always find the shortest path within the visibility graph [9]. The guarantee of the shortest path is the main justification, however, being able to handle local minima is important for more complicated scenarios where convex obstacles are not feasible.

Ultimately, the goal is to find the relationship between the cost ratio and uncertainty ratio, defined in section 1. Using Dijkstra's algorithm, the uncertainty ratio can be changed incrementally and the corresponding paths and cost ratios found. By plotting the cost ratio against the uncertainty ratio, figure 2, useful relationship characteristics can be found.

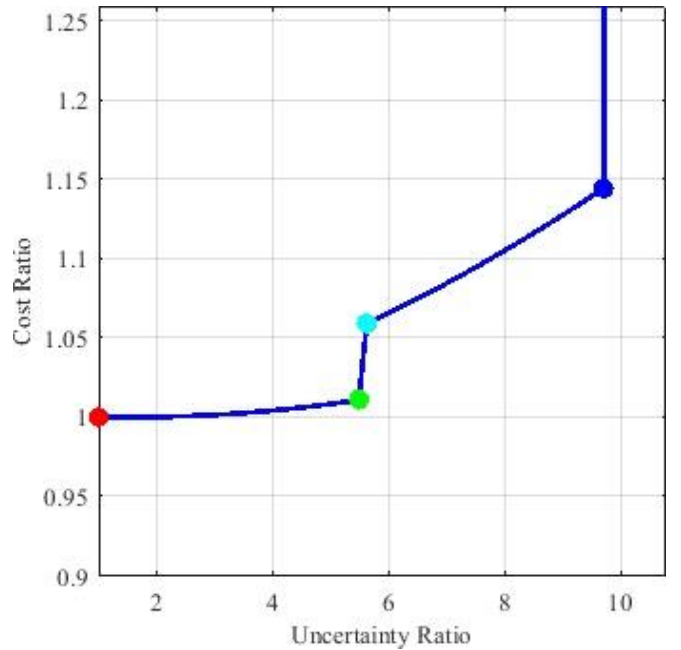


Figure 2: A sample cost ratio vs. uncertainty ratio plot for the corresponding map in figures 3 and 4. The colored dots correspond to the polytope colors in figures 3 and 4.

4. RESULTS

The first thing to observe from figure 2 is that the plots exhibit jumps in cost ratio at certain uncertainty ratios, caused by suddenly changing between different path options, which the authors refer to as “bifurcation points.” If the bifurcation

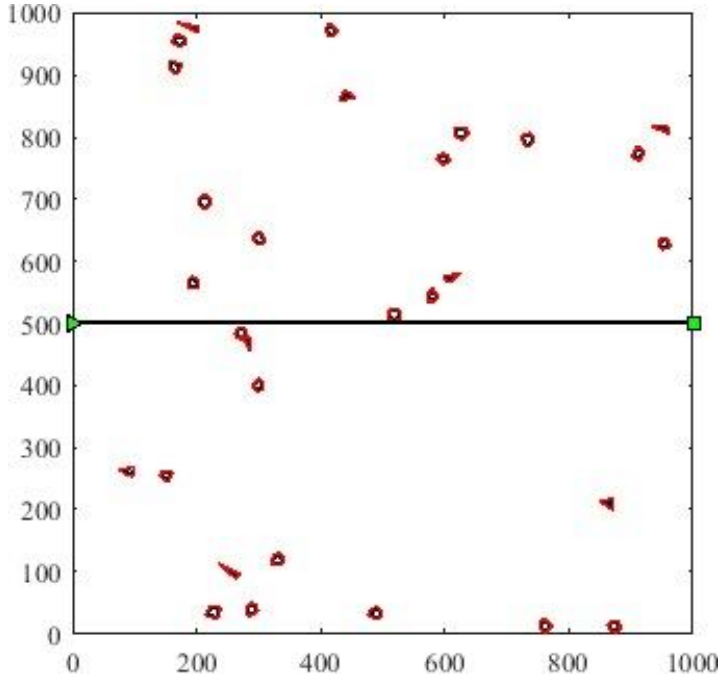


Figure 3: The ground truth obstacle map (black) with dilations for vehicle size (red). The units for this map are meters and the vehicle radius from the centroid was assumed to be 3 meters.

points are observed in conjunction with the corresponding map, it can be seen that the bifurcations always occur when objects in close proximity to the path merge: i.e. when “choke points” are closed off. This can be seen in figure 4, where the top two figures correspond to uncertainties immediately before and after a bifurcation. Notice that the path made a significant change at this point, explaining the large change in the cost ratio.

A useful characteristic of these plots is that the relationship between the bifurcation points is nearly linear and can be conservatively assumed to be linear. Figure 5 shows the first section of the cost vs. uncertainty plot shown in figure 2 before the bifurcation point. The dashed line shows a perfectly straight line between zero uncertainty and the uncertainty immediately before the bifurcation. It can be shown with some simple geometry and extensive algebra (appendix) that under some simple assumptions, the relationship between the uncertainty ratio and cost ratio can be assumed to

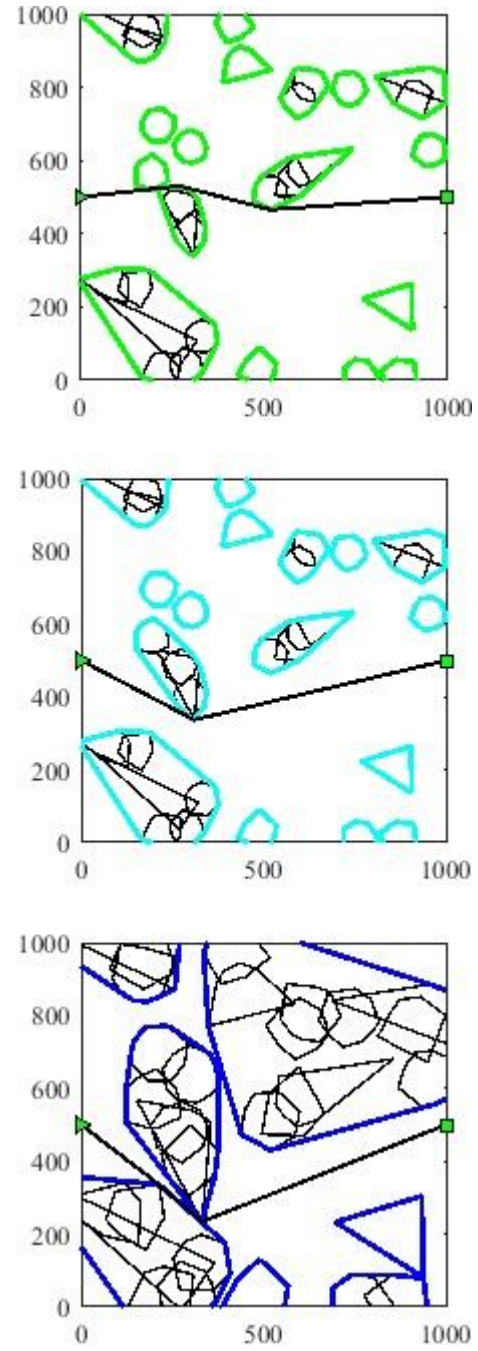


Figure 4: The top two maps show a choke point immediately before and after a bifurcation. The last plot shows the map before several polytopes merge and envelop the start point preventing further path planning. The black interior polytopes show the dilated obstacles before merging. Units are in meters.

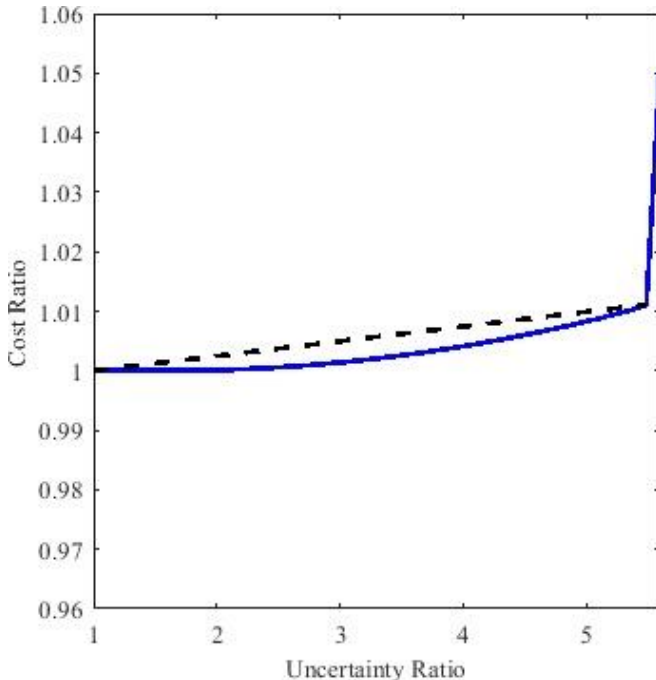


Figure 5: The relationship between bifurcation points is nearly linear.

be linear as the dashed line suggests. Additionally, the curve is always concave up meaning that the linear assumption is always conservative.

One note to make is that the plot goes to infinity at some uncertainty. This usually occurs because the start or goal point is either surrounded by obstacles, has no path out, or becomes enveloped by one of the expanding obstacles. This essentially means that the situation is now so uncertain that traversing the area is assumed to be impossible. Typically, this occurs at an uncertainty that is unrealistically high, but is worth mentioning here as it defines when the uncertainty is no longer increasing.

5. MODIFICATION FOR TURNING

The basic path planner returns a set of nodes that give a path of straight-line segments. However, most vehicles cannot make instantaneous turns especially at high speeds. To account for this, modifications to the point-to-point path-planner can be introduced to implement constant-radius cornering. The method for this is shown in figures

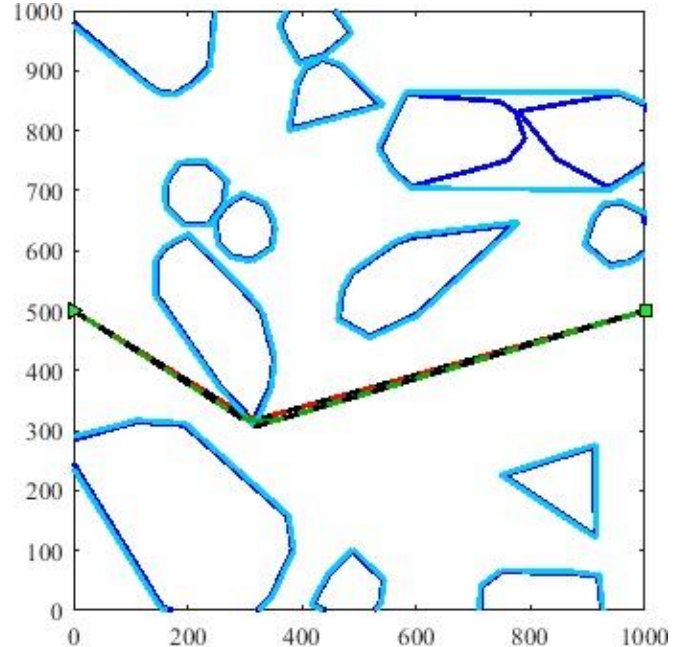


Figure 6: Example paths before and after arc correction. Units are in meters.

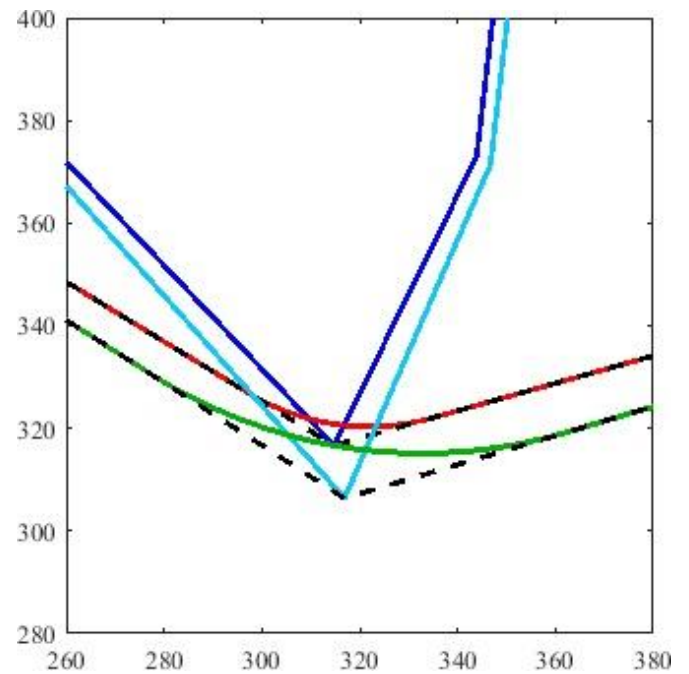


Figure 7: Zoomed-in portion of figure 6. The dark blue polytopes show the base obstacle and the lighter blue polytope shows the dilation of the obstacle to push the path away from the base obstacle. The dotted lines show the initial straight-line paths. The red and green paths show the arc path before and after correction respectively.

6 and 7. The original path (dashed) is planned and a radius equal to or greater than a vehicle's minimum turn radius is added at each line segment intersection. As figure 7 shows, this first path (red) cuts into the base polytope (dark blue), meaning the vehicle could collide with the obstacle. To prevent a vehicle collision, the polytope is dilated (light blue) further and the path re-planned, figure 7. This process can be repeated until a feasible path (green) is found. Methods other than obstacle dilation could be used for determining the turning radius adjustment. However, dilating an obstacle is a relatively quick calculation and lends itself to a

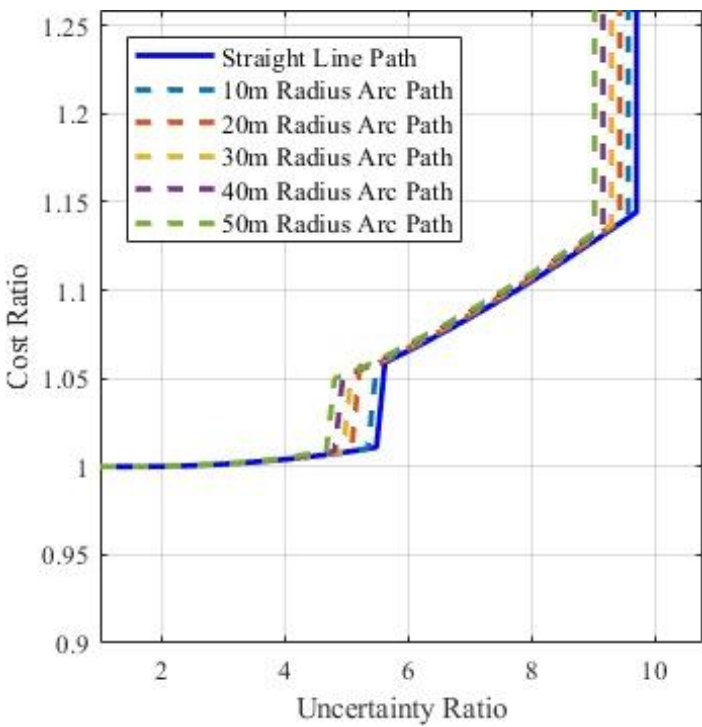


Figure 8: Straight line and arc path cost ratio vs. uncertainty ratio plots.

comparison between vehicle turning radius and additional uncertainty. This can be seen in figure 8 where additional vehicle turning radius results in a shift in uncertainty in the cost vs. uncertainty plot.

Although, the cost vs. uncertainty curve does change, as figure 8 shows, the major relationship characteristics still hold.

6. APPLICATION

The results found in this work lend themselves to several practical applications. The first is a fast method for determining the relationship between increasing uncertainty and path cost using the linear characteristic. If the relationship between bifurcations is assumed to be linear, then only the paths and associated costs at the bifurcation points need to be calculated and all the intermediate points can be approximated. To do this, the bifurcation points need to be identified. This can readily be done by first finding the initial path with the ground truth obstacles. Then the obstacles' uncertainty

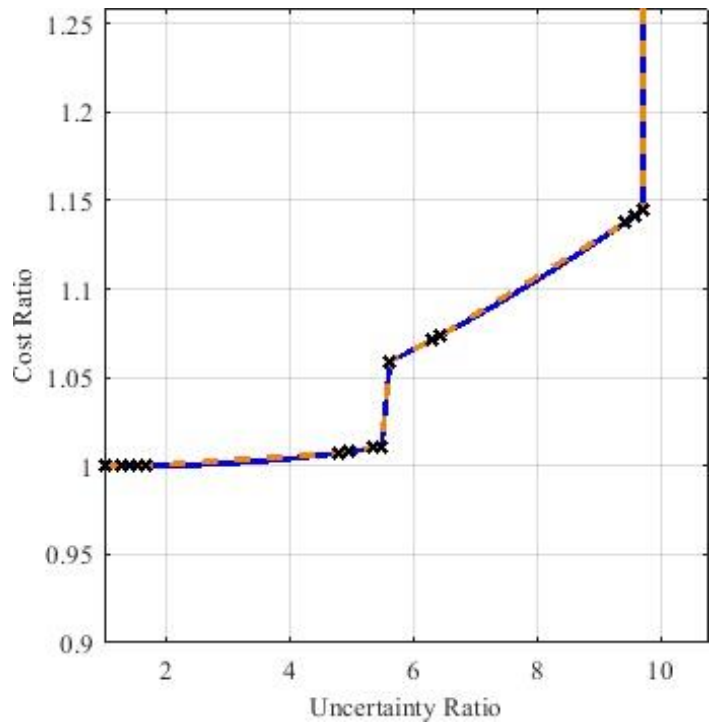


Figure 9: Straight line approximation of the cost ratio vs. uncertainty ratio plot.

should be increased until either a new obstacle impinges on the current path or one of the current vertices being used as a path point disappears due to obstacles merging. When either one of these happens, the path and cost at each point should be calculated. Once a path can no longer be calculated the points can be connected as shown in figure 9. The amount of calculation time reduction depends on several factors including the number of

uncertainty ratios considered, number of bifurcation points, bifurcation detection speed, and path planning speed. For the scenario presented here and the methods used by the authors, the calculation time was reduced by a factor of five.

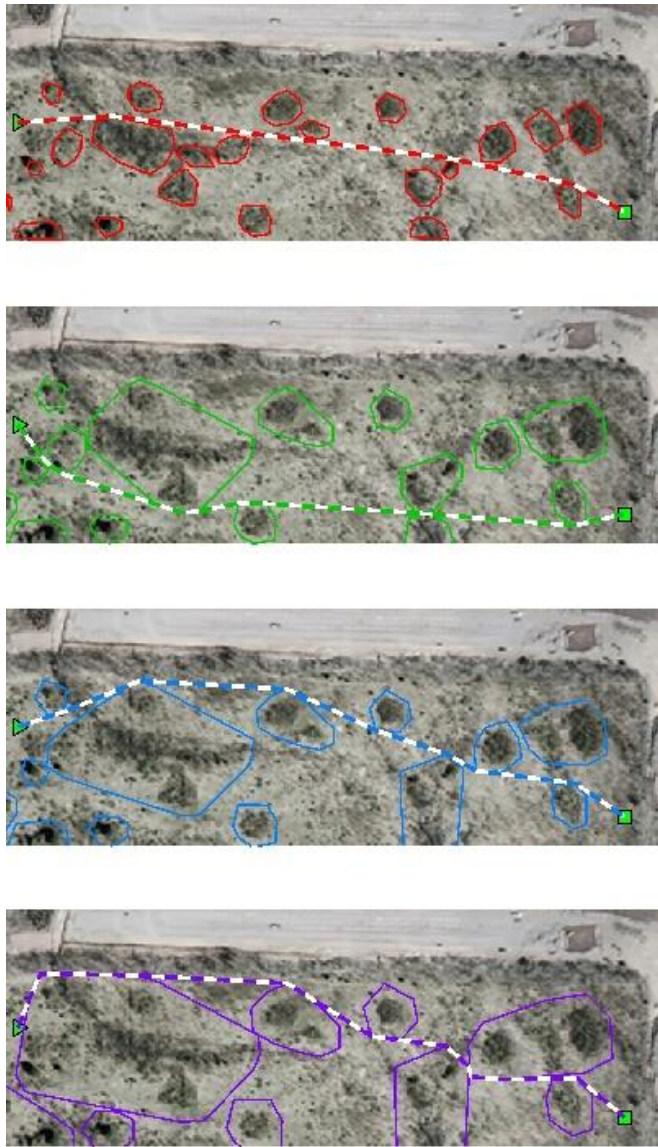


Figure 10: Example of path planning in a wooded area at the Keweenaw Research Center.

The second application is that map fidelity is really only needed to predict choke points; after objects are merged into larger convex polytopes, the fidelity of the map can be reduced. For example, the Keweenaw Research Center (KRC) has several

wooded areas, such as that shown in figure 10. If the choke points and the corresponding bifurcation points are identified the paths can be calculated at these points and the linear approximation described above can be used to describe the relationship for the given map entry and exit point, figure 11. At

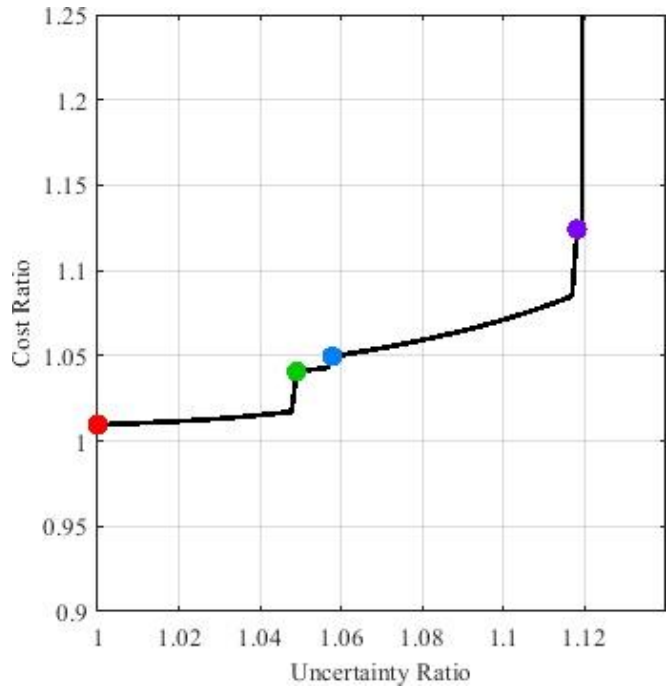


Figure 11: Cost ratio vs. uncertainty ratio plot for the wooded area. The colored dots correspond to the colors of the plots in figure 10.

that point, as long as the entry and exit point of the region are the same, the entire region can be described by one larger polytope that the vehicle can pass through at a cost described by the relationship in figure 11. If this were to be repeated for all reasonable entry and exit points to a given region, the interior of the region could be completely ignored, reducing the overall map fidelity.

Often times it may be found that taking a path through an obstacle field might be particularly costly, especially as costs other than distance are considered. In these cases, it may be more beneficial to stay on established road networks, as shown in figure 12. However, it may arise with some amount of rainfall over an extended period of

time that the bridge near the middle of the map may become washed out requiring a new, more costly, path to be calculated, figure 13. If the rain continues it may cause another previously traversed region to become impassable due to flooding, once again

requiring re-planning, as in figure 14. If the uncertainty is replaced with rainfall, a similar cost vs rainfall plot, figure 15, can be made and similar analysis can be done.



Figure 12: Planned path along the road networks and major drivable areas at KRC.

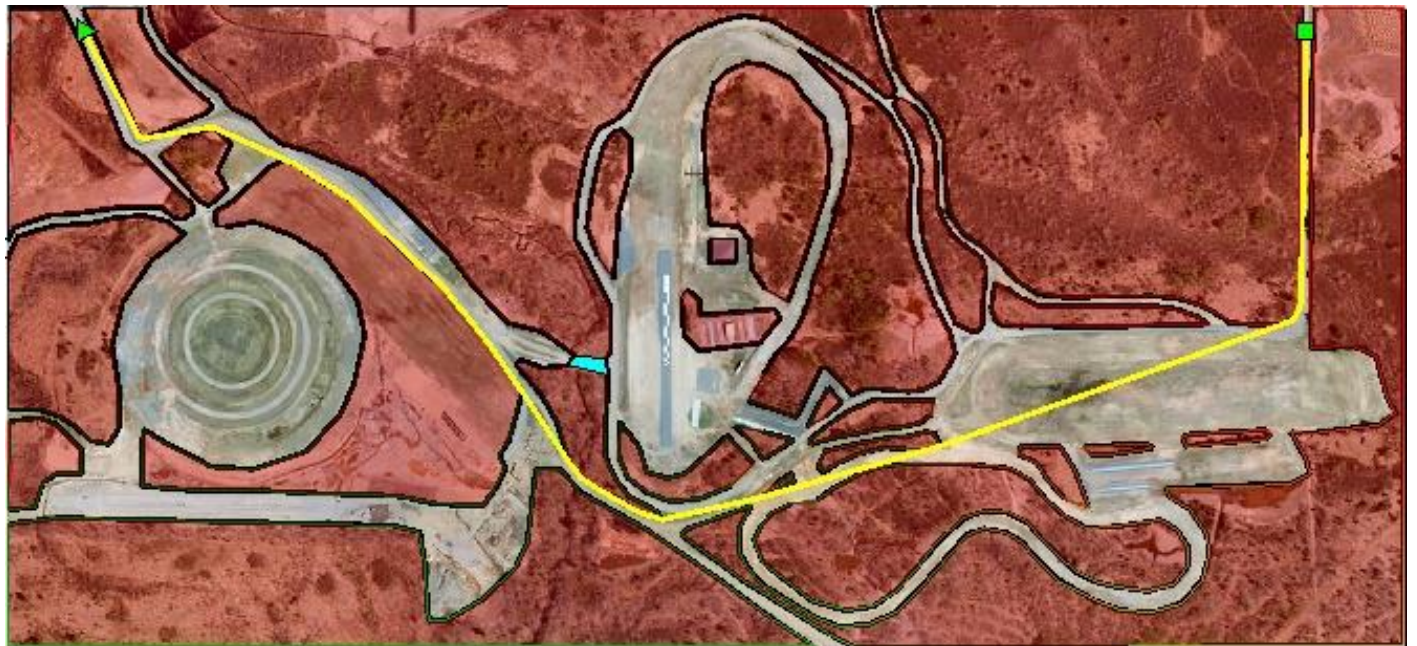


Figure 13: Planned path along the road networks and major drivable area at KRC with a washed-out bridge (light blue) at 2 inches of rain per hour.

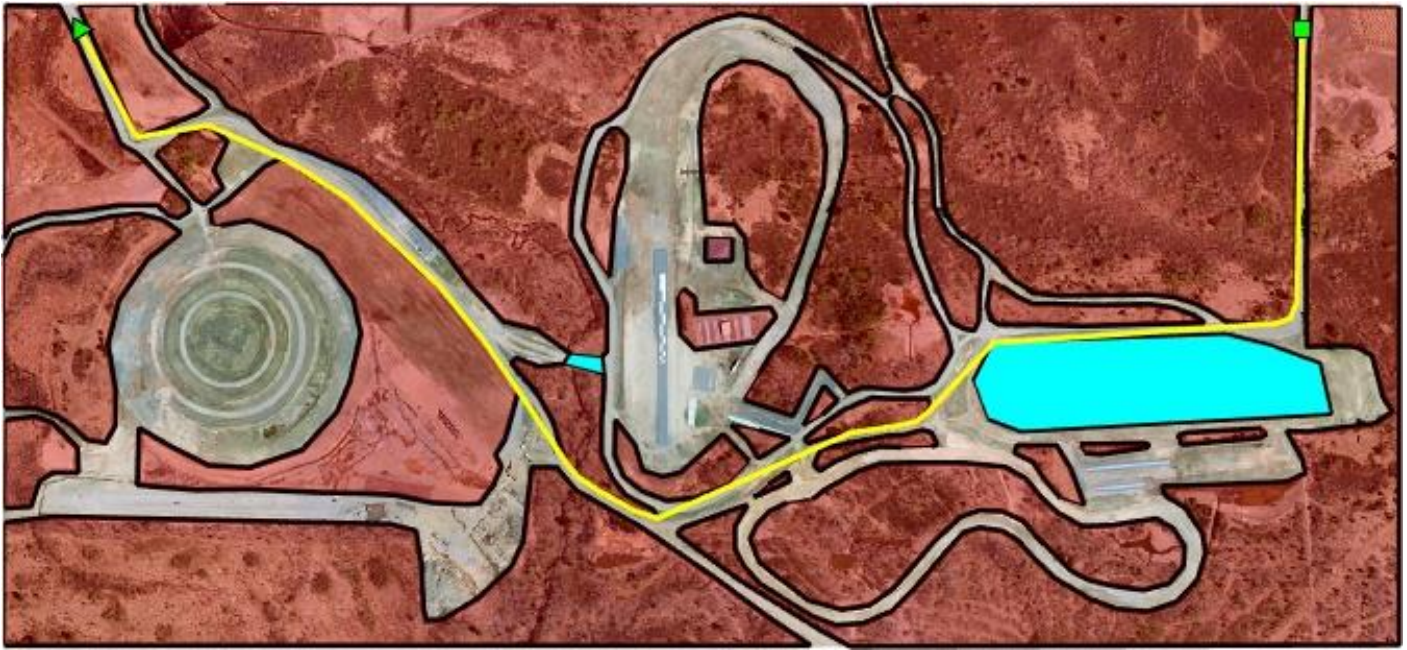


Figure 14 Planned path along the road networks and major drivable area at KRC with a washed-out bridge and flooded zone (light blue) at 4 inches of rain per hour.

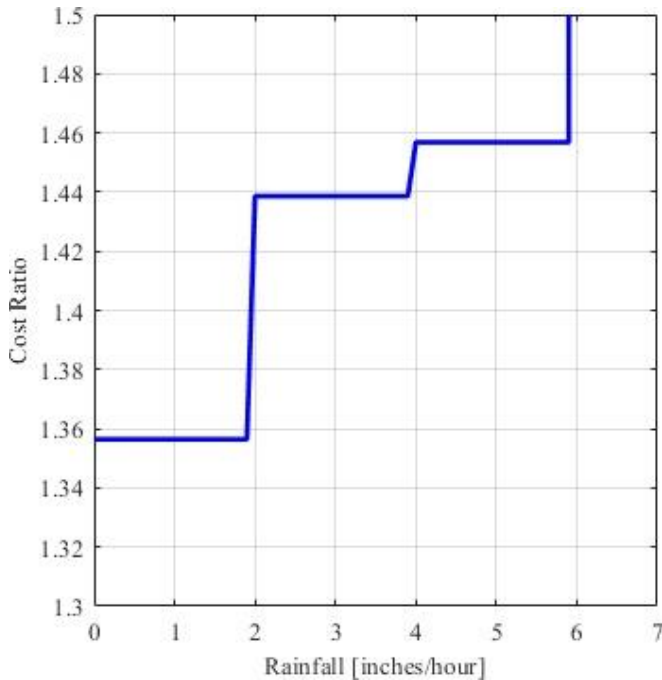


Figure 15: Example of what a cost ratio vs rainfall plot might look like for the scenario presented.

7. FUTURE WORK

As evident by the last application, the framework described here readily extends to other types of uncertainty such as terrain, soil, and rainfall, among others. Additionally, other costs could be used, such as traversal time, fuel use, or vehicle damage. It is the intent of the authors to work towards extending this framework to other costs and uncertainties.

The work here related cost to uncertainty for a specific map. However, if this type of analysis is done for many maps with similar characteristics, trends may become evident. If these trends are strong enough, they could be used to predict the cost to traverse a map without ever calculating a path. This could be a vital element for the NG NRMM.

1. REFERENCES

- [1] M. McCullough, P. Jayakumar, J. Dasch, and D. Gorsich (2017) "The Next Generation NATO Reference Mobility Model Development," *Journal of Terramechanics*, vol. 73, pp. 49-60
- [2] M. McCullough, J. Jayakumar, J. Dasch, and D. Gorsich, "Developing the Next Generation NATO Reference Mobility Model," in *NDIA Ground Vehicle Systems Engineering and Technology Symposium*, 2016.
- [3] M. Bradbury, J. Dasch, R. Gonzalez, H. Hodges, A. Jain, K. Iagnemma, M. Letherwood, M. McCullough, J. Priddy, B. Wojtysiak, and J. Y. Wong *Next Generation NATO Reference Mobility Model (NG-NRMM) Final Report by NATO Exploratory Team et-148*, Tech. rep., North Atlantic Treaty Organization.
- [4] K. K. Choi, N. Gaul, P. Jayakumar, T. M. Wasfy, and M. Funk, "Framework of Reliability-Based Stochastic Mobility Map for Next Generation NATO Reference Mobility Model," in *NDIA Ground Vehicle Systems Engineering and Technology Symposium*, 2018.
- [5] K. K. Choi, H. Cho, M.-Y. Moon, N. Gaul, D. Lamb, and D. Gorsich, "Confidence-Based Uncertainty Quantification and Reliability Assessment Using Limited Numbers of Input and Output Test Data and Validated Simulation Model," in *NDIA Ground Vehicle Systems Engineering and Technology Symposium*, 2017.
- [6] D. M. Ghiocel, D. Negrut, D. Lamb, and D. Gorsich, "An Integrated High-Performance Computing Reliability Prediction Framework for Ground Vehicle Design Evaluation," in *NDIA Ground Vehicle Systems Engineering and Technology Symposium*, 2009.
- [7] T. Lozano-Pérez and M. A. Wesley, "An Algorithm for Planning Collision-Free Paths Among Polyhedral Obstacles," *Communications of the ACM*, no. 22, 1979.
- [8] N. J. Nilsson, "A Mobile Automation: An Application of Artificial Intelligence Techniques," in *International Conference on Artificial Intelligence*, Washington, D.C., 1969.
- [9] M. B. Ignat'yev, F. M. Kulakov, and A. M. Pokrovskiy, "Robot manipulator control algorithms," Rep. No. JPRS 59717, NTIS, Springfield, Va., 1973.
- [10] P. E. Hart, N. J. Nilsson and B. Raphael, "A Formal Basis for the Heuristic Determination of Minimum Cost Paths," *IEEE Transactions of Systems Science and Cybernetics*, vol. 4, no. 2, pp. 100-107, 1968.
- [11] E. W. Dijkstra, "A note on two problems in connexion with graphs," *Numerische Mathematik*, vol. 1, no. 1, pp. 269-271, 1959.

2. Appendix

In order to show that the relationship between the cost ratio and uncertainty ratio is linear, we need to show that the length of the paths leading into each obstacle vertex changes linearly with the increase in obstacle size. Because both the cost ratio and uncertainty ratio are made unitless by dividing the path length and obstacle radius by constants, if the changes in path length (blue distance minus the green distance in figure 16) are linearly related to the dilation distance (distance between purple

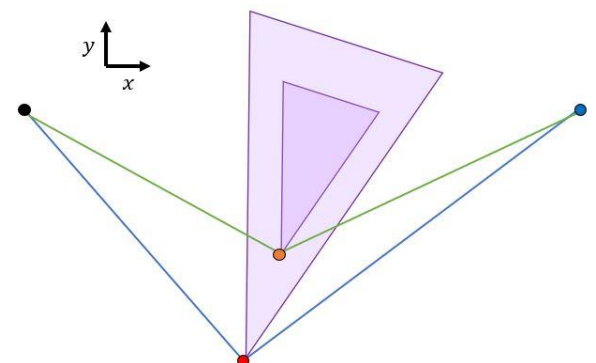


Figure 16: Dark purple obstacle expanding to lighter purple and the path adjusting from green to blue.

triangle edges), then the cost ratio and uncertainty ratio will also be linearly related.

This can be shown if the change in length is related by some constant to the expansion distance,

$$L_2 - L_1 = K_1 \delta + K_2$$

where L_1 is the original distance from the blue point at (x_0, y_0) to the original vertex (orange point) at (x_1, y_1) , L_2 is the distance from the blue point to the dilated vertex (red point) at (x_2, y_2) , δ is the dilation distance, and K_1 and K_2 are both constant, which are shown in figures 17 and 18.

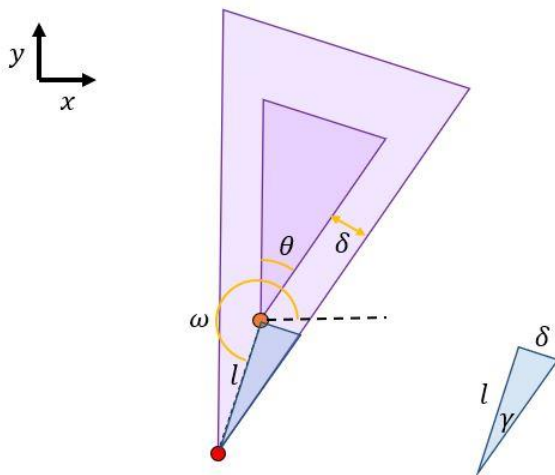


Figure 17: Length and angle definitions for the original and dilated polytopes.

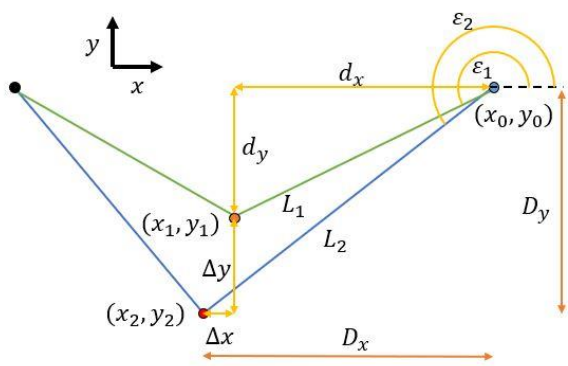


Figure 18: Length and angle definitions for the green and blue paths.

The change in the length can be derived in terms of the dilation distance,

$$L_2 - L_1 = \frac{D_x}{\cos(\varepsilon_2)} - \frac{d_x}{\cos(\varepsilon_1)}$$

where d_x is the x distance from the blue point to the orange point, D_x is the x distance from the blue point to the red point, ε_1 is the original angle of the connecting segment, and ε_2 is the dilated angle of the connecting segment.

The distance equation then becomes,

$$L_2 - L_1 = \frac{d_x + l \cos \omega}{\cos \varepsilon_2} - \frac{d_x}{\cos \varepsilon_1},$$

where l is the distance the vertex moved and ω is the angle defining the direction it moved.

We can define the second term as a constant since all terms within it are constant.

$$C = \frac{d_x}{\cos \varepsilon_1} = \text{constant}$$

We can find ε_2 in terms of an arc tangent of distances as

$$\varepsilon_2 = \tan^{-1} \left(\frac{D_y}{D_x} \right) = \tan^{-1} \left(\frac{d_y + l \sin \omega}{d_x + l \cos \omega} \right),$$

where d_y is the y distance from the blue point to the orange point and D_y is the y distance from the blue point to the red point.

Using the definition of the cosine of an arctangent and expanding the denominator we get

$$\begin{aligned} \cos(\varepsilon_2) &= \frac{d_x + l \cos \omega}{\sqrt{(d_y + l \sin \omega)^2 + (d_x + l \cos \omega)^2}} \\ &= \frac{d_x + l \cos \omega}{\sqrt{d_y^2 + 2d_y l \sin \omega + l^2 \sin^2 \omega + d_x^2 + 2d_x l \cos \omega + l^2 \cos^2 \omega}}. \end{aligned}$$

We can then substitute in some replacement variables for constants,

$$\cos \varepsilon_2 = \frac{d_x + l \cos \omega}{\sqrt{E + 2Bl + l^2}},$$

where $E = d_y^2 + d_x^2$ and $B = d_y \sin \omega + d_x \cos \omega$.

Substituting this back into the length equation and simplifying we get

$$L_2 - L_1 = \frac{d_x + l \cos(\omega)}{\left(\frac{d_x + l \cos(\omega)}{\sqrt{E + 2Bl + l^2}} \right)} + C$$

$$L_2 - L_1 = \sqrt{l^2 + 2Bl + E} + C.$$

We then use the fact that $l = \delta \cot(\gamma)$, where $\gamma = \frac{\theta}{2}$ and θ is the interior angle of the polytope at the vertex of interest to get

$$L_2 - L_1 = \sqrt{c^2 \delta^2 + 2Bc\delta + E} + C,$$

where $c = \cot\left(\frac{\theta}{2}\right) = \text{constant.}$

Using the definition of B , we can find that the largest B can ever become is $\sqrt{d_y^2 + d_x^2} = \sqrt{E}$. Substituting this for B we get the result

$$L_2 - L_1 = \sqrt{c^2 \delta^2 + 2\sqrt{E}c\delta + E + C}$$

$$= \sqrt{(c\delta + \sqrt{E})^2} + C = c\delta + \sqrt{E} + C$$

$$L_2 - L_1 = K_1\delta + K_2,$$

where $K_1 = c$ and $K_2 = \sqrt{E} + C$, which are both constant.

For every smaller value of B , the values drift farther from linear and closer to the square root of a quadratic. However, because the c^2 will always be positive, the quadratic will always be concave up, ensuring the linear approximation will always be conservative.

Acknowledgment:

This paper is based upon work supported by the Army Ground Vehicle Systems Center under Contract Number N00024-12-D-6404, Delivery Order Number #18F8346. The content of the information does not necessarily reflect the position or policy of the Government, and no official endorsement should be inferred.